Equilibrium vortex-line configurations and critical currents in thin films under a parallel field

Gilson Carneiro*
Instituto de Física, Universidade Federal do Rio de Janeiro, C.P. 68528, 21945-970, Rio de Janeiro-RJ, Brazil
(Received 23 July 1997)

Vortex-line equilibrium configurations and critical currents for type-II superconducting films at zero temperature are studied theoretically. The films are assumed to be of thickness less than or equal to the penetration depth, free of pinning by imperfections, and to be subjected to a magnetic field parallel to the film surfaces and to a transport current perpendicular to the field. By numerical minimization of the exact London-theory energy expression, using simulated annealing techniques, the equilibrium configurations are determined with great accuracy over a wide range of fields and currents. These consist of chains of straight vortex lines whose number depends both on the field and on the current. Transitions involving a change by one in the chain number are found to take place either if the field is increased at zero transport current or if the transport current is increased at constant field. At the transitions, there is a considerable rearrangement in the vortex-line positions and a small, discontinuous, change in their number. The equilibrium configurations with chain numbers that are not too small form a nearly perfect triangular lattice, centered with respect to the film surfaces. However, small deviations from this arrangement are found to be important in determining the behavior near the transition and when the transport current approaches the critical current. It is found that the critical current has a a nonmonotonic dependence on the field. The zero-temperature equilibrium phase diagram in the field-transport current plane is reported. [S0163-1829(98)08809-2]

I. INTRODUCTION

There is a great deal of activity nowadays in the investigation of the properties of the mixed state in type-II superconductors under various physical situations. One problem of interest is the study of vortices in films of thickness comparable with the penetration depth placed on an external magnetic field parallel to the film surfaces. In this case vortices enter the film as straight lines parallel to the field direction. The shielding current penetrates the full thickness of the film and pins the vortex lines to the film's interior. A transport current applied parallel to the film surfaces and perpendicular to the vortex lines will not dissipate energy unless its magnitude is large enough for the Lorentz force exerted by it on the vortex lines to overcome the force generated by the shielding currents and by the interactions between the vortex lines. Therefore, even in the absence of pinning by imperfections, the mixed state in the film can support a finite transport current without dissipating energy, that is in thermodynamic equilibrium.

Previous theoretical work on this problem has calculated, in the London limit, the equilibrium vortex-line configurations and critical currents using both analytical[1–5] and numerical[6] methods. These find that the equilibrium configurations consist of vortex-line chains and that there are transitions, induced by changing the applied magnetic field, in which the number of chains changes.

Measurements on films in this geometry of the magnetization and of the critical current have been reported by several authors.[6–12] It is found that the magnetization has peaks as a function of the field, not present in the bulk material, which are interpreted as resulting from the transitions involving the change in the number of chains.[6–8] Some of the critical current measurements find nonmonotonic dependence on the field that is also attributed to these transitions.[9–11] Other measurements find no such dependence, but the large critical currents observed are interpreted as due to pinning of the vortex lines by the shielding current.[12]

The aim of this paper is to calculate in detail the vortex-line equilibrium configurations and critical currents at zero temperature in films of thickness less than or equal to the penetration depth, without pinning by imperfections, in the presence of both a parallel field and a transport current. The starting point of this calculation is the known expression for the energy of a system of straight vortex lines parallel to the film surfaces, exact in the London limit for sufficiently thin films.[1–6] Minimization of this energy is carried out numerically, using simulated annealing techniques, assuming only that the distributions of vortex lines in the film is periodic. By this method the equilibrium vortex-line configurations are determined very accurately over a wide range of external fields and transport currents. Several results are reported.

The equilibrium configurations obtained by this method are found to consist of vortex-line chains, all with the same intrachain spacing between vortex lines. In the absence of a transport current, it is found that, as the external field grows above the lower critical field, there are regions where the number of chains remains constant in which the number of vortex lines in the film grows smoothly with the field. Transitions consisting of a change by one of the number of chains are found to take place at critical field values. These results are consistent with previous ones, obtained using a similar numerical method.[6] The present calculation reveals that at the transitions, besides the considerable rearrangement in the vortex-line positions found previously,[6] their number has a small discontinuous increase. Even for a modest number of chains, the equilibrium vortex-line configurations are found to be close to a triangular lattice, as predicted in Refs. 2 and

3. However, it is found that there are significant differences between the triangular lattice and the equilibrium configurations, not reported previously, that play an important role in the vicinity of the above described transitions. The changes in the equilibrium vortex-line configurations caused by a transport current are studied in detail and the critical current is calculated. It is found that by changing the transport current at constant field up to the critical current, two distinct behaviors take place, depending on the field value. In the first the number of chains remains the same as that for no current. The effects of the current are to shift the chains towards the film surface and to slightly increase the number of vortex lines. Near the critical current this shift is nonuniform, contrary to previous calculations that find a uniform shift.[2] It is found that if the vortex chains were forced to shift uniformly, a critical current considerable larger than that obtained from the exact calculation would result. The second type of behavior is one in which, as the current grows past a certain value, smaller than the critical current, a transition to a configuration with one additional chain takes place. This is similar to the transition that occurs by increasing the field without a transport current and has not been predicted in previous calculations. The critical current versus field curve is found to be nonmonotonic with a structure that is a direct consequence of the vortex-line-chain configurations that exist in the film. The zero-temperature equilibrium phase diagram in the external field-transport current plane is obtained.

This paper is organized as follows. In Sec. II the London theory results for the energy are briefly reviewed. In Sec. III the numerical method for energy minimization is presented. In Sec. IV the results obtained by this method are reported and their physical significance is discussed. Finally, in Sec. V the predictions of this paper are compared to experiment and its conclusions stated.

II. LONDON THEORY

Consider a film made of a type-II superconducting material of thickness D, length L, and width L. The material is assumed to be uniaxially anisotropic, with anisotropy axis perpendicular to the film surfaces (the c axis) and characterized by anisotropy parameter γ ($\equiv\sqrt{m_{ab}/m_c}$). The other material parameters are the penetration depth λ, for currents flowing parallel to the a-b plane, and the coherence lengths in the a-b plane ξ.

The film is assumed to be subjected to an external field H parallel to the film surfaces (along the b direction) and to a transport current flowing perpendicular to H and also parallel to the film surfaces (a direction), whose average current density is J_t (Fig. 1).

The interest here is to obtain the equilibrium vortex-line configurations and the critical currents at zero temperature for $D\leqslant\lambda$, in the London limit, $\lambda\gg\xi$. It is assumed that (i) the vortex lines are straight and parallel to the field direction (b direction). (ii) Their distribution in the ac plane is periodic in the a direction, with period a_v. This periodic structure consists of L/a_v identical primitive unit cells with dimensions $D\times a_v$ placed side by side. Each cell contains n_v vortex lines located at (x_{aj},x_{cj}), $j=1,2,\ldots,n_v$, with $0\leqslant x_{aj}<a_v$ and $0\leqslant x_{cj}\leqslant D$ (Fig. 1). Even though these assumptions allow for very general vortex-line configurations, the calculations reported here find that the equilibrium ones consist of n_v chains of vortex lines located at $\{x_{cj}\}$, with vortex lines uniformly spaced from one another within each chain by a_v (Fig. 1).

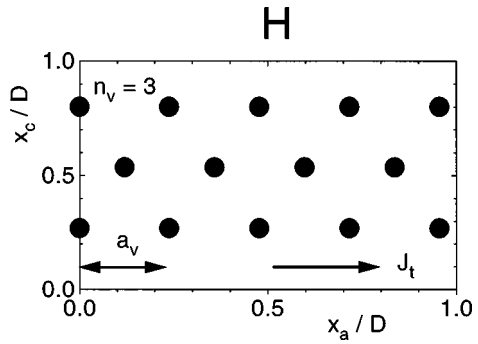

FIG. 1. A portion of the film cross section showing a typical vortex-line configuration. The primitive unit cell is indicated by the double arrow. The field H is entering the paper (b direction). The transport current direction is indicated by the single arrow.

The solutions of London equations for the film with an arbitrary distribution of straight vortex lines parallel to the film surface were obtained by several authors using the method of images.[1–6] One such vortex line, with vorticity $q=1$ and located at (x_a,x_c) $(D\geqslant x_c\geqslant 0)$, generates two infinite sets of mirror images. One set has images with vorticity $-q$ located at $-x_c+2nD$, $n=0,\pm1,\pm2,\ldots$. The other has images with vorticity q located at x_c+2mD, $m=\pm1,\pm2,\ldots$.

The total energy of an arbitrary distribution of such vortex lines can be written as

$$E=E_{\rm int}+E_{\rm self}+E_H+E_J. \tag{1}$$

In Eq. (1) $E_{\rm int}$ is the energy of interaction of vortex lines with one another and with the images, excluding the self-images; $E_{\rm self}$ is the vortex line self-energy plus the energy of interaction with their own images; E_H is the energy of interaction of the vortex lines with the screening current generated by the external field, and E_J is the energy of interaction of the vortex lines with the transport current.

For an isotropic film ($\gamma=1$), and in the limit where $(\pi\lambda/D)^2\gg1$, $E_{\rm int}$ and $E_{\rm self}$ are given by

$$E_{\rm int}/L^2=\epsilon\frac{1}{2a_v}\sum_{n,i,j}\ln\left[\frac{\cosh\,\pi(na_v+x_{ai}-x_{aj})/D-\cos\,\pi(x_{ci}+x_{cj})/D}{\cosh\,\pi(na_v+x_{ai}-x_{aj})/D-\cos\,\pi(x_{ci}-x_{cj})/D}\right], \tag{2}$$

where $\epsilon=(\phi_0/4\pi\lambda)^2$ and $\Sigma_{n,i,j}$ runs over $n=0,\pm1,\ldots,\pm L/a_v$, and $i,j=1,2,\ldots,n_v$, excluding for $n=0$ the $i=j$ term;

$$E_{\rm self}/L^2=\epsilon\frac{1}{2a_v}\sum_{j=1}^{n_v}\ln\left[\frac{4\sin^2(\pi x_{cj}/D)+(\pi\xi/D)^2}{(\pi\xi/D)^2}\right]. \tag{3}$$

The energies of interaction with the currents are given by

$$E_H/L^2=\epsilon\frac{4\pi\lambda^2 H}{\phi_0 a_v}\sum_{j=1}^{n_v}\left[\frac{\cosh(x_{cj}-D/2)/\lambda}{\cosh D/2\lambda}-1\right], \tag{4}$$

and

$$E_J/L^2=\epsilon\frac{8\pi^2\lambda^2 D J_t}{\phi_0 a_v c}\sum_{j=1}^{n_v}\left[\frac{\sinh(x_{cj}-D/2)/\lambda}{\sinh D/2\lambda}+1\right]. \tag{5}$$

The total energy for an anisotropic film ($\gamma\neq1$) is related to that for an isotropic film ($\gamma=1$), with the same λ and D, by the following scaling relation:[13]

$$E[\xi,a_v,\{(x_{aj},x_{cj})\},H,J_t;\gamma]=\gamma E[\gamma\xi,\gamma a_v,\{(\gamma x_{aj},x_{cj})\},\gamma^{-1}H,\gamma^{-1}J_t;\gamma=1]. \tag{6}$$

Thus the equilibrium configurations for an anisotropic superconductor follow from the corresponding ones for the isotropic material by scaling the parameters according to Eq. (6). In what follows the discussions will be limited to isotropic materials.

In order to obtain the equilibrium vortex-line configuration it is necessary to find the minimum of E, Eq. (1), for given H and J_t. This is discussed next.

III. ENERGY MINIMIZATION

The energy minimization is carried out numerically using simulated annealing. For a given H and $J_t=0$, the following procedure is used. Assuming that there are n_v vortex lines within the unit cell, a standard Monte Carlo (MC) procedure that moves vortex lines within a single cell is used to find the positions (x_{aj},x_{cj}) and cell length a_v at a given ''temperature.''[14] This fictitious temperature is used to overcome energy barriers. By lowering it the minimum of E/L^2, Eq. (1), is found. The equilibrium configurations are obtained from this data by comparing the minimum energies for different n_v and determining the lowest one.

For $J_t\neq0$ it is necessary to search for a local minimum of E/L^2, Eq. (1), at fixed n_v. The reason is that for fixed n_v and for $J_t>0$, E is unbound because vortex lines placed at $x_c=D$ have zero interaction energy and self-energy, but negative E_J. Thus the energy can always be lowered by putting more and more vortex lines at $x_c=D$ close together. The local minimum is, clearly, the physically relevant one.

For given H and n_v the local minimum is determined as follows. Starting from the vortex-line configuration found for these values of H, n_v, and for $J_t=0$, a new configuration that minimizes E is determined for small J_t by running the MC procedure at very low ''temperature.'' This avoids ''thermal'' fluctuations that might overcome the energy barrier separating the local minimum from the unphysical configurations described above. By further increasing J_t by small amounts new local minima configurations are found. The equilibrium configurations for $J_t>0$ are determined as in the case where $J_t=0$, described above, by comparing the energies of the local minima for different n_v. It is found that above a certain value of J_t the vortex lines accumulate at $x_c=D$, their number growing without limit. This mimics what happens above the critical current, where vortex lines enter the film at $x_c=0$, are dragged by the transport current to the film surface at $x_c=D$, and are annihilated. The smallest value of of J_t where this happens is interpreted as the critical current J_c. This method allows the equilibrium configurations of interest to be determined accurately using small values of n_v and with modest personal computers.

In the results reported in Sec. IV λ and ξ are considered as fixed lengths. Films with $\xi=10^{-2}\lambda$ and $D=\lambda$, $\lambda/2$, $\lambda/4$ are investigated over a wide range of values of H and J_t. According to Eq. (1), for these values of D, E is weakly dependent on λ. The mathematical derivation of Eq. (2) requires only that $(\pi\lambda/D)^2\gg1$, which is satisfied.

The natural units for the external field and for the transport current are the lower critical field H_{c1} and of the depairing current J_d, respectively. For the films with $D\leqslant\lambda$ these quantities are given by

$$H_{c1}=\frac{\phi_0}{\lambda^2}\frac{\ln(2D/\pi\xi)}{4\pi(1-1/\cosh D/2\lambda)}, \tag{7}$$

and

$$J_d=\frac{1}{12\sqrt{3}\pi^2}\frac{c\phi_0}{\xi\lambda^2}. \tag{8}$$

For the films studied here the values of H_{c1} in units of ϕ_0/λ^2 are $H_{c1}(D=\lambda)=2.92$, $H_{c1}(D=\lambda/2)=9.04$, and $H_{c1}(D=\lambda/4)=28.37$.

IV. RESULTS AND DISCUSSION

For $J_t=0$, and for H just above H_{c1}, the equilibrium configuration is a single vortex chain ($n_v=1$) located at the film center (Figs. 2 and 3). As H increases the vortex lines in the chain come close together, that is a_v decreases, as shown in Fig. 4. Eventually a value of H is reached where the single chain splits in two chains ($n_v=2$), located symmetrically about the film center (Figs. 2 and 3). This two-chain configuration exists over a range of H values, above which the energy minimum corresponds to three chains ($n_v=3$) (Figs. 2 and 3). As H is further increased the pattern is as follows. A stable n_v-chain configuration occurs over a range of H, followed by a n_v+1-chain configuration as H grows past a critical value. At the $n_v\rightarrow n_v+1$-transition a_v increases discontinuously, with the amplitude of the discontinuity decreasing with increasing n_v (or H), as shown in Fig. 4. Similar results are obtained for other D values.

In Fig. 5 the total number of vortex lines per unit length of the film n_v/a_v is shown as a function of H. It is seen that the number of vortex lines increases roughly linearly with H, with constant slope in the regions where n_v is constant. At the $n_v\rightarrow n_v+1$ chain transition there is a discontinuous jump

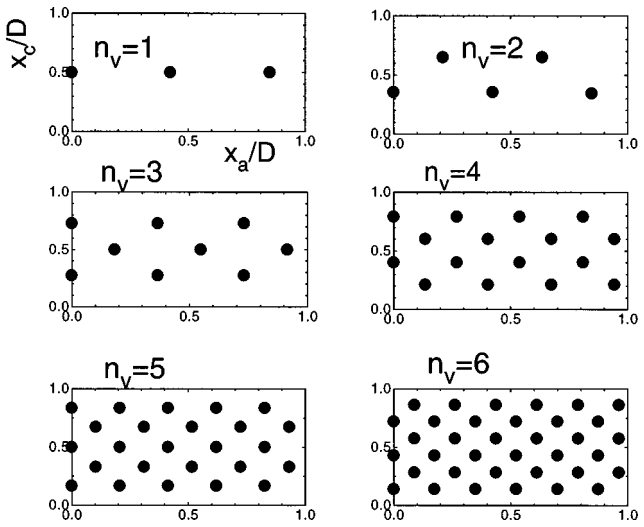

FIG. 2. Equilibrium configurations for $J_t=0$ and $D=\lambda$. The field values are: $H=2H_{c1}$ for $n_v=1$; $H=3H_{c1}$ for $n_v=2$; $H=5H_{c1}$ for $n_v=3$; $H=7.25H_{c1}$ for $n_v=4$; $H=11H_{c1}$ for $n_v=5$, and $H=15H_{c1}$ for $n_v=6$.

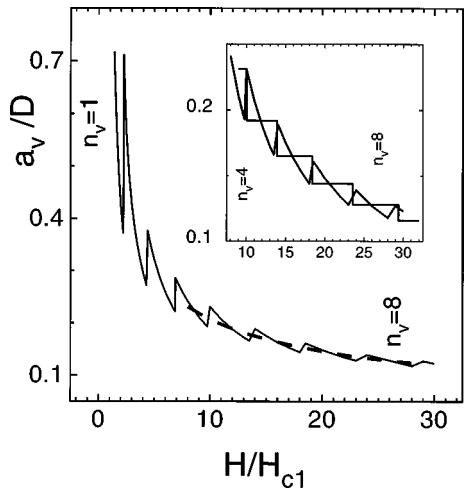

FIG. 4. Intrachain vortex-line spacing for $J_t=0$ and $D=\lambda$. Thick line: full minimization of E/L^2. Dashed curve: continuous approximation. Inset: comparison with the centered triangular lattice approximation (thin line). Both approximations are described in the text.

in n_v/a_v, by about 10% in the region covered by Fig. 5. The relative size of the discontinuities in both a_v and n_v are considerably larger (Fig. 4). However, these quantities increase by about the same factor so that the relative increase in their ratio is smaller. At higher values of H/H_{c1} than those shown in Fig. 5 the number of vortex lines continues to increase in the same fashion, but the discontinuity at the transitions become smaller.

Even for modest values of n_v, the equilibrium configurations are found to be very close to a perfect triangular lattice centered with respect to the film's surfaces (Fig. 6), as predicted in Refs. 2 and 3. However, the vortex-line configurations obtained by numerical minimization of Eq. (1) show important differences with this triangular lattice, as discussed next.

In the centered triangular lattice the distance between adjacent chains is $d_c=D/(n_v+1)$, which is also the distance from the first and last chains to the film surfaces at $x_c=0$ and $x_c=D$, respectively, and $a_v=d_c/\sin 60$ (Fig. 6). The results of the present calculation show that the chain spacing increases slightly towards the film center. Numerical minimization of E, Eq. (1), assuming a centered triangular lattice

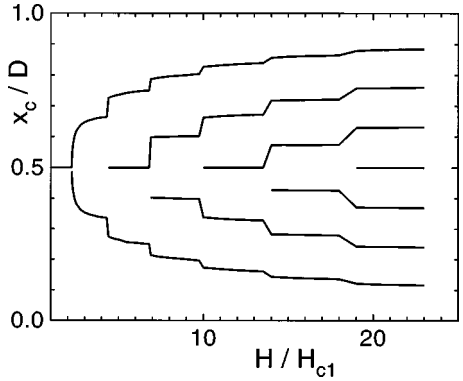

FIG. 3. Vortex-chain positions for $J_t=0$ and $D=\lambda$. The continuous lines are just guides to the eye.

structure, gives the $a_v\times H$ curve with steps shown in Fig. 4. In this approximation $a_v\simeq D/(n_v \sin 60)$, and n_v depends on H through the minimization of E/L^2. Consequently, a_v is independent of H in the range where n_v is constant, in sharp disagreement with the results described above. However, it is apparent from Fig. 4 that the triangular lattice prediction agrees well with the mean value of a_v in the range where n_v is constant. At the $n_v\rightarrow n_v+1$ chain transition d_c and a_v decrease discontinuously to fit a centered triangular lattice with n_v+1 chains. This leads to a $(n_v/a_v)\times H$ curve with steps: n_v/a_v is constant in the range where both n_v and a_v are constant and increases discontinuously by $\Delta(n_v/a_v)\simeq 2n_v \sin 60/D$ at the transition. This linear dependence on n_v of $\Delta(n_v/a_v)$ is also in strong disagreement with the results of the full minimization of Eq. (1), discussed above.

A simpler way to estimate n_v and a_v for large n_v is as follows. First replace the discrete vortex distribution by a continuous one $\nu_v(x_c)$ (=number of vortex lines per unit

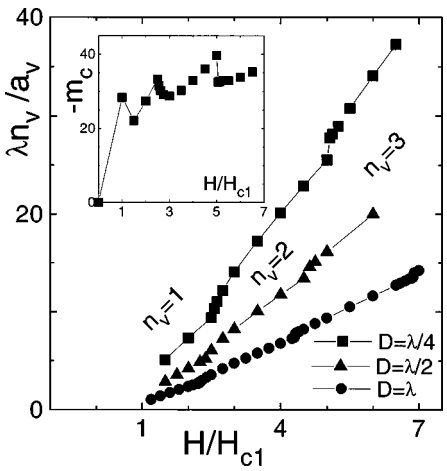

FIG. 5. Number of vortex lines per unit length in the film for $J_t=0$. Inset: magnetization along the c direction for $D=\lambda/4$ and $J_t=0$.

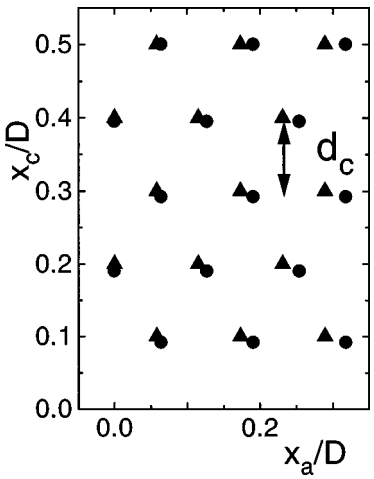

FIG. 6. Circles: vortex-line configuration for $H=30H_{c1}$, $n_v=9$, $J_t=0$, and $D=\lambda$, obtained from full minimization of E/L^2. Triangles: centered triangular lattice for $n_v=9$. The configurations are symmetric with respect to $x_c/D=0.5$

area). Minimization of Eq. (1) under this assumption gives

$$\nu_c(x_c)=\frac{H}{\phi_0}\frac{\cosh(x_c-D/2)/\lambda}{\cosh D/2\lambda}. \tag{9}$$

This result shows that the vortex-line density is slightly larger near the film's surfaces, in accordance with the results of the full minimization of Eq. (1), as discussed above. Next we approximate the average vortex-line density, n_v/a_vD, by the average over the film thickness of $\nu_c(x_3)$ which, according to Eq. (9) is $\overline{\nu_c}=(H/\phi_0)(2\lambda/D)\tanh(D/2\lambda)$, and use for a_v the centered triangular lattice approximation discussed above. For $n_v\gg 1$ this gives $n_v=D/(a_v\sin 60)$ and

$$a_v=\left[\frac{2\lambda H\sin 60}{D\phi_0}\tanh\frac{D}{2\lambda}\right]^{-1/2}. \tag{10}$$

This prediction agrees well with the average of a_v in the interval where n_v is constant, even for modest values of n_v, as show in Fig. 4. It shows that this average value decreases with $H^{-1/2}$. However, this approximation overestimates n_v in the range shown in Fig. 4.

For $D\leqslant\lambda$ the magnetic induction

$$B=\frac{\phi_0}{a_vD}\sum_{j=1}^{n_v}\left[1-\frac{\cosh(x_{cj}-D/2)/\lambda}{\cosh D/2\lambda}\right], \tag{11}$$

resulting from the vortex-line configurations in the field is small. It follows from Eq. (11) that $B\sim\phi_0(n_v/a_vD)(D/\lambda)^2/12$. Consequently, $M=(B-H)/4\pi$ deviates very little from the Meissner-state value $M=-H/4\pi$.

For $J_t>0$, and if H is not too close to the field where the $n_v\rightarrow n_v+1$ chain transition takes place at $J_t=0$, the equilibrium vortex configuration has the same n_v as that for $J_t=0$ and the same H. The chain positions are shifted towards the film surface located at $x_c=D$, a_v decreases slightly and, consequently, the number of vortex lines in the film increases a little. The shift grows with J_t and is nonuniform, with the chain closest to the film surface at $x_c=D$ shifting the most, as shown in Fig. 7. In this figure it is seen that as $J_t\rightarrow J_c$ the

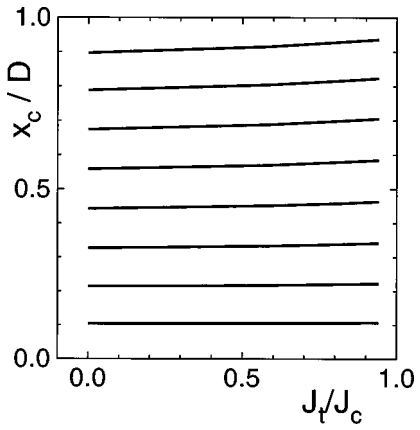

FIG. 7. Vortex-chain positions for $D=\lambda$ and $H=28H_{c1}$ ($n_v=9$).

chain closest to the $x_c=D$ film surface is about halfway between its position at $J_t=0$ and this surface.

A simple model to calculate J_c, proposed in Ref. 2, is to assume that the vortex lines form a rigid triangular lattice. In this case the effect of the force exerted by the transport current on the vortex lines is to displace the lattice uniformly towards the film surface. Equilibrium is reached when this force is balanced by that exerted by the other vortices and by the shielding current. Numerical calculations based on this model and on Eq. (1) show that above a critical value of J_t the rigid lattice has no equilibrium position within the film. However, this critical value is found to be considerably larger than that calculated as previously described. This shows that at least for the range of H values studied here, the subtle changes in the vortex-line configuration away from the triangular lattice caused by J_t play an important role in determining the critical current.

If H is close to the field for the $n_v\rightarrow n_v+1$ chain transition at $J_t=0$, it is found that a similar transition takes place by increasing J_t at constant H. The vortex-line structure in the film can be summarized in a zero-temperature equilibrium phase diagram, as shown in Fig. 8. For $D=\lambda/2$ and $D=\lambda/4$ the phase diagram is similar. The critical currents for these D values are shown as a function of H in Fig. 9.

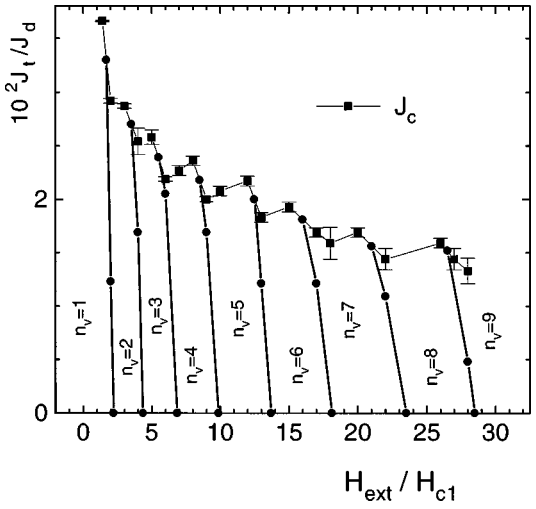

FIG. 8. Zero-temperature equilibrium phase diagram for $D=\lambda$.

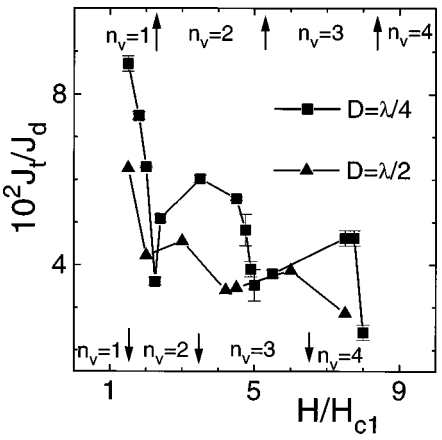

FIG. 9. Critical currents. The arrows on the upper (lower) axis mark the range over which n_v has the value indicated for $D=\lambda/4$ ($D=\lambda/2$).

V. CONCLUSIONS

The calculations reported in Sec. IV describe the behavior of an ideal model, that is, vortex lines in equilibrium at zero temperature in films without imperfections under a field that is precisely parallel to the film surfaces. Even a very small angle between the field and the film surfaces, which is always present in experiments, invalidates these predictions, since dissipation occurs when $J_t \neq 0$. In such fields the vortex lines are tilted. The Lorentz force exerted by J_t on these lines has a component along the b direction which will move the lines and dissipate energy. However, since the tilt is small, it takes only a small amount of pinning to prevent this motion. Morever, it is reasonable to assume that the tilted vortex-line configurations are very close to those for untilted vortex lines at the same field. That is, the vortex lines are nearly parallel to the b direction and their average positions in the ac plane coincide with those obtained for lines parallel to the b direction. Thus, the ideal model predictions are applicable to equilibrium properties of films, provided only that pinning by imperfections is sufficiently weak and that the field makes a small angle with the film surfaces.

It has been usual to relate peaks in the magnetization data on films with the $n_v \rightarrow n_v+1$ chain transitions that occur in the ideal model.[6–8] It is therefore interesting to discuss what are the predictions of the ideal model for the behavior of the magnetization.

As discussed in Sec. IV, the magnetization due to vortex lines that are exactly parallel to the film surfaces deviates very little from the Meissner value. If the vortex lines are tilted with respect to the b direction the equilibrium magnetic induction has a c component B_c. Assuming that the tilt is uniform, B_c is proportional to the number of vortex lines per unit area, that is $B_c \propto \phi_0(n_v/a_v D)$. The equilibrium magnetization has also a c component $M_c \propto \phi_0(n_v/a_v D - H/\phi_0)$. Thus, M_c is a direct measure of number of vortex lines in the film. In Fig. 5 (inset) $m_c = -(n_v/a_v D - H/\phi_0)\lambda^2$ is plotted versus H. The peaks seen in this figure result from the increase in the number of vortex lines in the film that take place at the $1 \rightarrow 2$ and $2 \rightarrow 3$ chain transitions. Similar results are obtained for larger values of D. Experiments on Nb/Cu multilayers reported in Refs. 6–8 find that the $M_c \times H$ curve has peaks at field values approximately equal to those where the $n_v \rightarrow n_v+1$ chain transition takes place in the ideal model. If these experiments measure the equilibrium M_c, there is the following disagreement with the ideal model predictions. The experimental $|M_c|$ decreases in the range of H where n_v is constant, whereas the ideal model predicts that it increases. If in the experimental setup the vortex lines in the film are not in equilibrium, then it is unclear how the M_c peaks are related to a transition that only takes place in equilibrium.

In the experiments reported in Refs. 6–8 M_c is measured as H is changed at $J_t=0$. According to the results reported above, the $n_v \rightarrow n_v+1$ chain transition can also take place if J_t is increased at constant H. This suggests that if peaks in M_c are indeed related to the $n_v \rightarrow n_v+1$ chain transitions, it may be possible to observe peaks in M_c by increasing J_t at constant H.

The measurements of the critical current in films under a parallel field reported in Refs. 9–12 can also be compared to the ideal model predictions. The main characteristics of these predictions are a nonmonotonic $J_c \times H$ dependence and values of $J_c \sim 1 - 9 \times 10^{-2} J_d$. The results reported in Refs. 9–11 show nonmonotonic dependence on H, with characteristic features at H values comparable to those where a $n_v \rightarrow n_v+1$ chain transition takes place. However the critical currents measured in Refs. 9 and 11 are one order of magnitude smaller than those predicted by the present calculation. The results reported in Ref. 12 show only a monotonic dependence on H, and find J_c values that are about one order of magnitude larger than those shown in Figs. 8 and 9.

In conclusion then, the ideal model predictions are not fully supported by the experimental data. However, this model is useful as a starting point to study the interesting behavior of films with weak pinning under parallel fields. Further work is necessary in order to incorporate into the model the effects that are neglected here.

ACKNOWLEDGMENTS

It is a pleasure to thank Professor M. Doria for stimulating conversations. This work was supported in part by FINEP/Brazil, CNPq-Brasília/Brazil and Fundação Universitária José Bonifácio.

*Electronic address: gmc@if.ufrj.br

[1] C. Carter, Can. J. Phys. **47**, 1447 (1969).

[2] V. V. Shmidt, Zh. Éksp. Teor. Fiz. **57**, 2095 (1969) [Sov. Phys. JETP **30**, 1137 (1970)]; **61**, 398 (1971) [**34**, 211 (1972)].

[3] A. I. Rusinov and G. S. Mkrtchyan, Zh. Éksp. Teor. Fiz. **61**, 773 (1971) [Sov. Phys. JETP **34**, 413 (1972)].

[4] Y. Mawatari and K. Yamafuji, Physica C **228**, 336 (1994).

[5] S. Takáks, Czech. J. Phys., Sect. B **33**, 1248 (1983); **36**, 521 (1986); **38**, 1050 (1988).

[6] S. H. Brongersma, E. Verweij, N. J. Koeman, D. G. de Groot, R. Griessen, and B. I. Ivlev, Phys. Rev. Lett. **71**, 2319 (1993).

[7] J. Guimpel, L. Civale, F. de la Cruz, J. M. Murduck, and I. K. Schuller, Phys. Rev. B **38**, 2342 (1988).

[8] M. Ziese, P. Esquinazi, P. Wagner, H. Adrian, S. H Brongersma,

and G. Griessen, Phys. Rev. B **53**, 8658 (1996).
[9] T. Yamashita and L. Rinderer, J. Low Temp. Phys. **24**, 695 (1976).
[10] N. Ya. Fogel' and V. G. Cherkasova, Fiz. Nizk. Temp. **7**, 268 (1981) [Sov. J. Low Temp. Phys. **7**, 131 (1981)], and references therein.
[11] P. Lobotka, I. Vávra, R. Senderák, D. Machajdí, M. Jergel, Š. Gaži, E. Rosseel, M. Baert, Y. Bruynseraede, M. Forsthuber, and G. Hilscher, Physica C **229**, 231 (1994).
[12] G. Stejic, A. Gurevich, E. Kadyrov, D. Christen, R. Joynt, and D. C. Larbalestier, Phys. Rev. B **49**, 1274 (1994).
[13] G. Blatter, M. V. Feigel'man, V. B. Geshkenbein, A. I. Larkin, and V. M. Vinokur, Rev. Mod. Phys. **66**, 1125 (1994).
[14] See, e.g., *Monte Carlo Methods in Statistical Physics*, edited by K. Binder (Springer, Berlin, 1979).